Available online at www.sciencedirect.com
SCIENCE DIRECT®
Quaternary International 121 (2004) 13–22

Modelling of the erosion in the Rhone valley during the Messinian crisis (France)

J. Gargani

École Nationale supérieure des Mines de Paris, Laboratoire de Sédimentologie-CGES, rue St-Honoré, Fontainebleau, F-77300, France

Abstract

A geometric reconstruction of the present day Messinian Rhone valley shows two slope breaks. After taking into account the post-Messinian tectonics and Messinian isostatic compensation due to deep valley incision and Mediterranean Sea unloading, these two slope breaks were still visible on the reconstructed original Messinian Rhone profile. One is located on the Cevennes fault system and the other one is downstream of St-Marie. The slope of the ante-Messinian profile was approximately 0.05%.

The Messinian Rhone profile was simulated using a numerical erosional model based on mass conservation. The Messinian profile cannot be explained only by variations of erosional processes such as lithology or changes in discharge, and one has to consider that the Messinian crisis happened in two phases. The profile of the Rhone was in steady state just after the first Messinian phase of lowering.The amplitude of the sea level lowering is around 600 m for the first phase, whereas the amplitude of the second one is 1300–1700 m. The isostatic deformation during the Messinian crisis due to bedrock erosion and sea unloading produced important changes in the Mediterranean dynamic.

1. Introduction

The important dimension of the Messinian Rhone canyon is a fundamental element in understanding the evolution of the Mediterranean Sea. The origin of the Messinian salinity crisis is a question that has given rise to controversy: Tectonic (Rouchy, 1981; Krijgsman et al., 1999) or eustatic controls (Cita, 1973; Clauzon, 1982) have been proposed. The Messinian salinity crisis occurred over a period of 450–630 ky [5.8–5.32 million years BP (Baumard, 2001), 5.96–5.33 million years BP (Krijgsman et al., 1999)]. It left deep incision profiles in the main rivers flowing into the Mediterranean Sea (Fig. 1).

The lowering of the Mediterranean Sea during the Messinian crisis has been estimated at 500–1000 m (Mauffret, 1979; Durand Delga, 1980), 1500 m (Schlupp, 2001), 2500 m by several authors (Le Pichon et al., 1971; Ryan and Cita, 1978; Clauzon, 1982), and 3000 m (Malinverno et al., 1981). The large amplitude of the erosion and the well-defined chronology of the Mediterranean lowering make it a unique example for testing erosional models on fluvial systems. But the precise history of the Mediterranean sea is always an unresolved question.

This study is based on a precise reconstruction of the Messinian Rhone valley over a large region, taking into account post-Messinian tectonic and isostatic deformation due to the important incision and to sea unloading. The resulting paleoprofile is used to explore the genesis of the Messinian Rhone valley. An erosion model is applied in order to assess the pre-Messinian Rhone valley and to quantify the erosion during the Messinian crisis.

2. Messinian Rhone profile

2.1. Present day geometric reconstruction

The present day river profile used in this study is a reconstruction of the paleovalley of the Messinian Rhone from Lyon to the Mistral drilling (~350 km) based on seismic data, drilling data and field observations. The width of the studied area varies from 35 km near Lyon to 146 km near Sainte-Marie de la Mer. The paleovalley has been reconstructed with the geological model *gocad* (Figs. 2 and 3) (Colson et al., 2000).

The 3D geometric reconstruction was used to build a profile of the Messinian Rhone River (Fig. 4). The obtained profile shows two main slope breaks whereas

E-mail address: julien.gargani@ensmp.fr (J. Gargani).

1040-6182/$ - see front matter © 2004 Elsevier Ltd and INQUA. All rights reserved.
doi:10.1016/j.quaint.2004.01.020

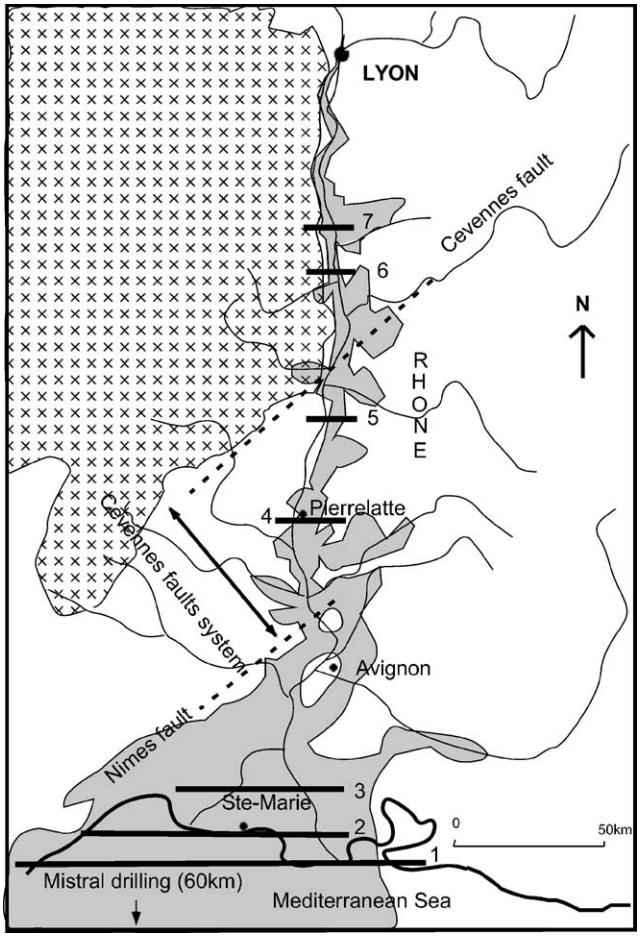

Fig. 1. Pliocene deposits of the Messinian Rhone valley, France (from Ballesio, 1972). Grey: Pliocene filling. Crosses: Granit basement.

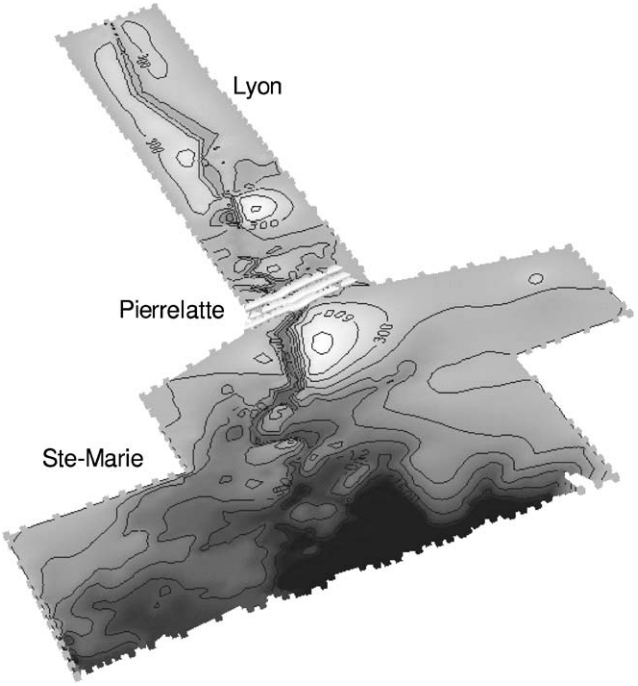

Fig. 2. Present day geometric reconstruction of the Messinian Rhone valley. Light to dark gray: decreasing altitude (Colson et al., 2000).

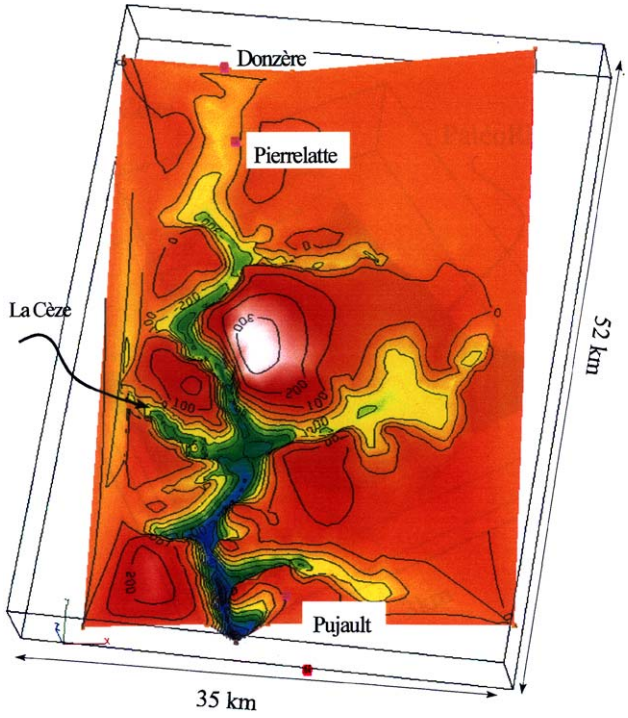

Fig. 3. Present day geometric reconstruction of the Messinian Rhone valley. Detail (Colson et al., 2000).

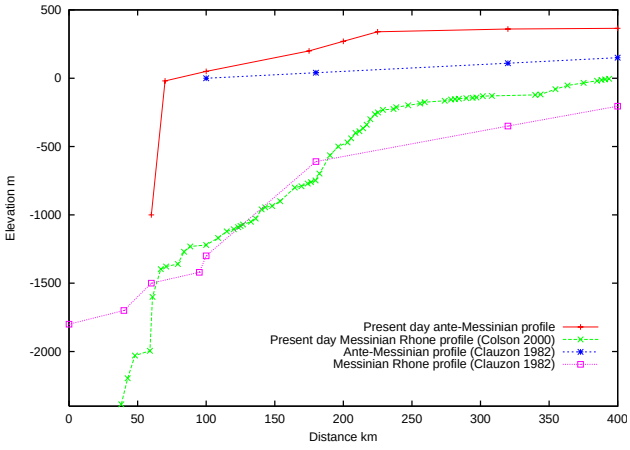

Fig. 4. Present day reconstructed profile of the Messinian Rhone river and ante-Messinian profile by Colson 2000. Comparison with the results of Clauzon 1982. The results of Clauzon are not presented with the present altitudinal referential. (He supposed that the slope of the initial profile is 0.05%. From the amplitude of the Messinian incision, he reconstructed the Messinian Rhone profile).

the former profile published based on less control points had only one (Clauzon, 1982). Other smaller differences in the thalweg elevations result from the density of information taken into account.

2.2. *Influence of post-Messinian tectonics*

Firstly, the influence of the post-Messinian deformation on the present day reconstructed profile was

investigated. Most of the results are based on the work of Mandier (1988) on post-Messinian vertical deformation along the middle Rhone profile: (1) at the north of the Cevennes fault system (defined as the system from the Cevennes fault to the Nimes fault), an uplift of around 40 m is estimated during the Rhodanian phase (upper Miocene) and around 225 m of homogeneous uplift are attributed to the Plio-Quaternary, (2) within the Cevennes fault system, an average uplift of 145 m has been identified during the Plio-Quaternary. In the southern part of the Cevennes fault system, 40 m of post-Messinian vertical uplift have been estimated, as a maximum, on the Nimes fault (Schlupp et al., 2001). In the offshore region, the post-Messinian sediment pile is apparently not deformed by tectonics. The morphology of the continental margin is essentially controlled by gravity flow processes (Bellaiche et al., 1984, 1988). Regional subsidence of the offshore region is generally admitted, but the quantification of this subsidence is not precisely determined (Kooi et al., 1992).

Taking into account these elements, a profile was reconstructed which corresponds to the present day erosion surface of the Messinian Rhone with a differential vertical translation of the profile of 265 m in the north and an average vertical translation of 145 m in the Cevennes fault system. The present day ante-Messinian Rhone profile was also reconstructed taking into account the post-Messinian uplift. At first, the Gulf of Lyons subsidence was not taken into account because the quantification is still a subject of discussion.

The restored profile shows that post-Messinian tectonic deformations have enhanced the amplitude of the Pierrelatte knick point by ~265 m, while the downstream profile is not deformed (Fig. 5). Nevertheless, on the restored profile the knickpoint is still present although associated with a slope break of lesser amplitude.

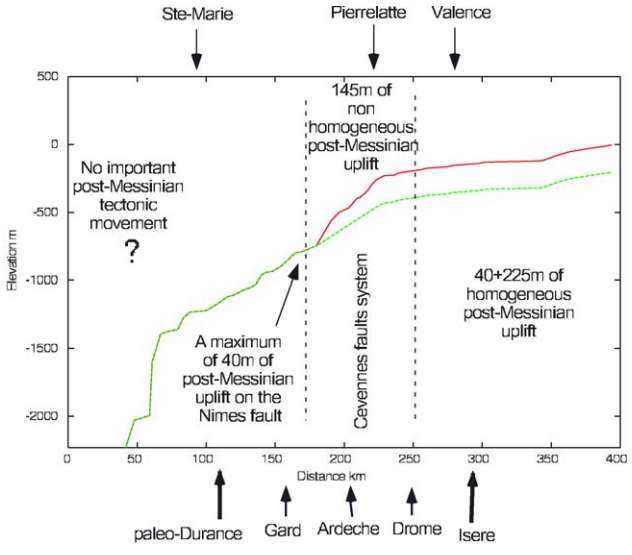

Fig. 5. Messinian Rhone profile before (upper one) and after (lower one) taking into account post-Messinian deformation. Lower arrows indicate probable locations of the paleo-tributaries (bold: important flow).

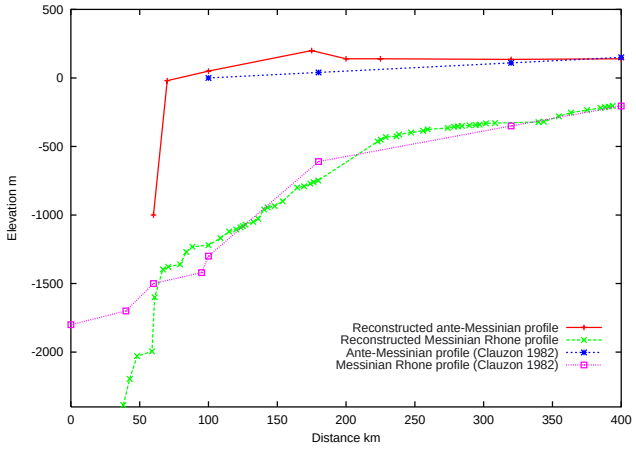

Fig. 6. Reconstructed profile of the Messinian Rhone river and ante-Messinian profile taking into account post-Messinian tectonic. Comparison with Clauzon results.

These results can be compared with those of Clauzon (1982) (see Fig. 6). The results confirm the hypothesis of Clauzon (1982) of an initial slope of ~0.05%. The Messinian profile is deeper downstream of Sainte-Marie than is the Clauzon profile. A recent study confirms our result downstream of Sainte-Marie (Guennoc et al., 2000).

3. Erosional processes

Various equations have been used for modelling erosional processes: the mass conservation equation, the stream power equation (Howard et al., 1994; Montgomery, 1994), the Universal Soil Loss Equation, the Water Erosion Prediction Project (Nearing and Nicks, 1998), and semi-empirical or phenomenological equations (Perrin et al., 1993; Kooi and Beaumont, 1994). Because the mass conservation equation has been used in an important number of studies (Culling, 1960; Begin et al., 1981; Thomas, 1982; Willgoose et al., 1991; Pelletier and Turcotte, 1997; Allen and Densmore, 2000) and is a well established physical model, we choose to use it in our simulation. There is ample literature on the different applications of this equation and on the analytical and numerical methods to solve it (Carslow and Jaeger, 1959). The theoretical basis of the continuity equation assures the possibility to study the influence of the second order processes such as lateral mass supply (Begin et al., 1981), tectonics (Willgoose et al., 1991), autocyclic dynamics in fluvial sedimentary basin (Pelletier and Turcotte, 1997), and variations of sediment flow in response to the climatic

variations (Veldkamp and van Dijke, 2000). The simplest form of this equation is

$$\delta z/\delta t = 1/\gamma_s \times \delta Q_s/\delta x, \quad (1)$$

where z is the altitude, γ_s is the bulk weight per unit volume of sediment, and x is the longitudinal distance. It is often considered that sediment flow Q_s is linearly proportional to the slope (Culling, 1960; Begin et al., 1981):

$$Q_s = k_1 \delta z/\delta x \quad (2)$$

with

$$k_1 = C_1 Q_W(\gamma_W^3 f/8g)^{1/2}, \quad (3)$$

where C_1 is an empirical constant, Q_w is the water discharge per unit charge, γ_w is the water density, f is the Darcy–Weisbach factor and g is the acceleration due to gravity. Substituting (2) into (1) yields a simple erosion law formulated as

$$\delta z/\delta t = K\delta^2 z/\delta x^2, \quad (4)$$

K is a coefficient of erodability, with dimension L^2/T. Eq. (4) can be numerically calculated.

4. Isostatic compensation

The isostatic consequences of deep erosion and Mediterranean Sea unloading on the longitudinal river profile were also investigated. The erosion transformed an originally undeformed lithosphere in isostatic equilibrium to a configuration which is not in isostatic equilibrium. Thus isostatic restoring stresses will immediately act to regain isostatic equilibrium (Weissel and Karner, 1989). The lithospheric deformation depends on the quantity of material eroded, but also of the mechanical property of the crust. In the classical model of a thin elastic plate, the mechanical parameters are the Young's modulus E, the Poisson's ratio v and the effective elastic thickness T_e which determine the flexural rigidity D:

$$D = ET_e^3/12(1 - v^2). \quad (5)$$

Flexural rigidity values are often considered to be between 10^{20} and 10^{24} N m (Weissel and Karner, 1989; King and Ellis, 1990; Pazzaglia et al., 1998).

5. Ante-Messinian Rhone profile

The first run of the erosional model was performed considering a smooth slope (~0.05%) for the ante-Messinian Rhone profile as shown in Fig. 6, and a sea level lowering of 2200 m during 450 ky for the Messinian crisis (Fig. 7). Modelling was then conducted on the restored Messinian profile taking into account the post-Messinian deformation but without considering Messinian isostatic compensation. The resulting profile shows only one slope break (Fig. 8). It is impossible to interpret, using only these hypotheses, the complexity of the Messinian Rhone profile. In order to model the two slope breaks the influence of the parameters controlling the coefficient of erosion k and the influence of the two phases of the Mediterranean Sea lowering were investigated.

5.1. Erosion coefficient

5.1.1. Influence of lithology

Variations of the coefficient of erosion are linked to lithological changes or flow variations. Based on geological maps, a clear change in lithology can be identified north of the Cevennes fault system, around 175–200 km from the present shore line (near Sainte-Marie),

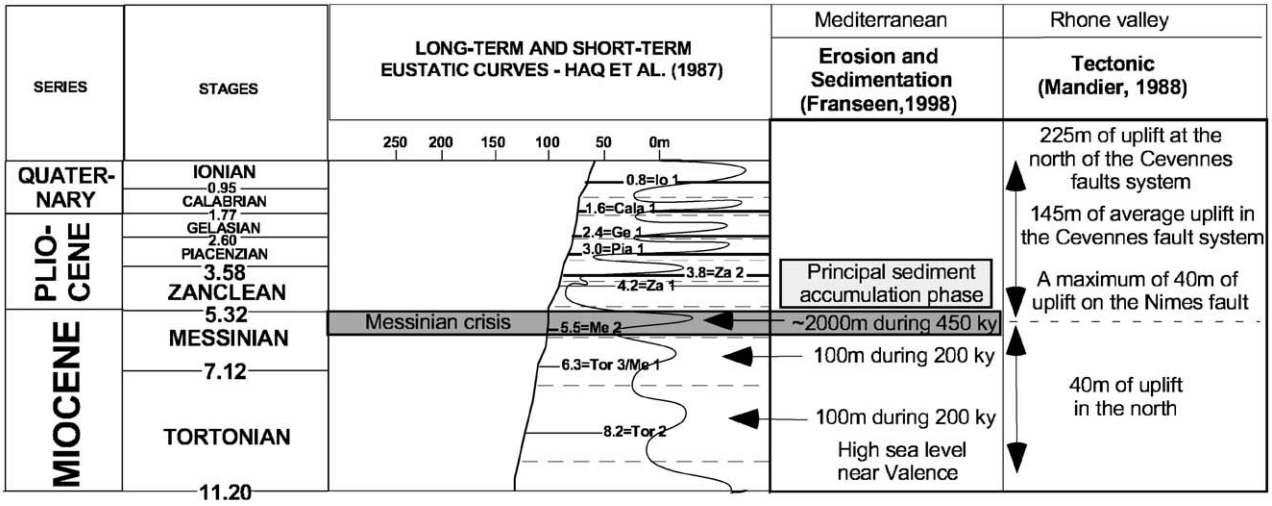

Fig. 7. Timing and amplitude of sea level variation in the Mediterranean sea in comparison to the global eustatic curve. Tectonics affecting Rhone river is also indicated.

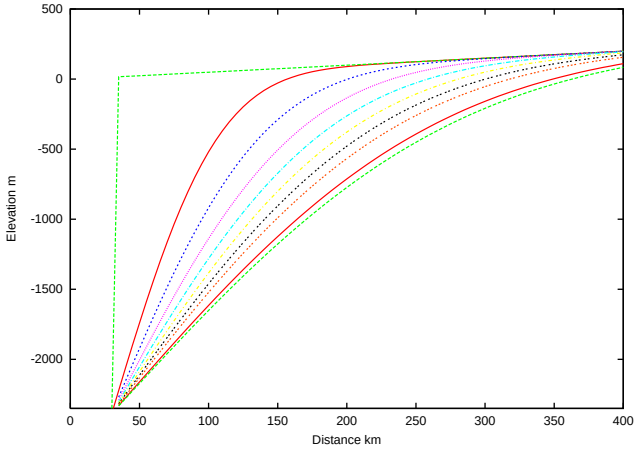

Fig. 8. Evolution with time of the river profile using mass conservation equation. $K = 35\,000\,m^2$/year. Profiles are represented every 50 000 years. Initial slope is of 0.05%.

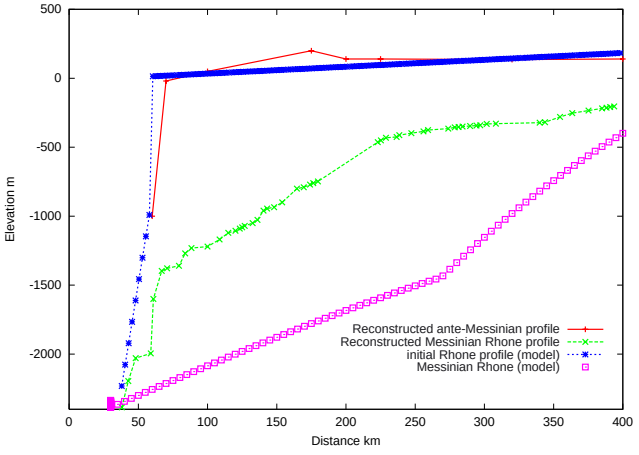

Fig. 9. Influence of the coefficient of erodibility K. If $x < 250$ km, $K = 50\,000\,m^2$/year and if $x > 250$ km, $K = 150\,000\,m^2$/year.

with a substrate dominated by basement rocks to the north and sedimentary rocks to the south (Fig. 1). Differences in the lithology are simulated by changes in the erosion coefficient. For resistant rocks, the coefficients of erosion are small. Two models with different values for the coefficient of erosion were tested. In the first test the lithology was supposed to be less resistant downstream (Fig. 9). In this case, the model does not fit the reconstructed profile. The second test, assumed that the lithology was more resistant downstream (Fig. 10). The model fits the reconstructed profile, but the supposed lithology is not realistic.

Lithological change can not lead to the Messinian Rhone profile. Thus, lithological changes were not the cause of the two knick points of the Rhone profile.

5.1.2. *Influence of river flow*

The variation of the flow induced by tributaries may modify the coefficient K along the profile. Although the

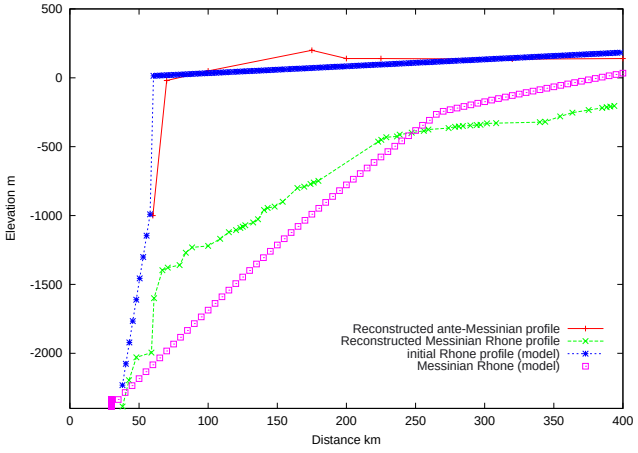

Fig. 10. Influence of the coefficient of erodibility K. If $x < 250$ km, $K = 150\,000\,m^2$/year and if $x > 250$ km, $K = 50\,000$ m2/year.

Messinian reconstruction of the Rhone network is not fully documented, geological observations confirm the existence of a paleo-Durance (south of the present Durance), a paleo-Isere (north of the present Isere) and certainly of a paleo-Gard (Fig. 1). The Pliocene deposits in the Messinian incised valley of the paleo-tributaries of the Rhone are not located in the same place as the present tributaries. The geometry of the Messinian hydrological network can be considered in studying the possible influence on the Rhone profile of the rivers flowing into the Rhone.

Messinian Rhone profile analyses do not allow quantification of the possible influence of the two most important rivers flowing into the Rhone: the paleo-Durance and the paleo-Isere. At the resolution scale of the profile there is no significant influence of river flows on the Messinian Rhone profile. Furthermore, the inferred location of the confluence does not fit with the knick point locations (Fig. 5). The influence of longitudinal flow variations along the Rhone profile does not determine knick point location.

6. Quantification of the two phases of sea level lowering

From the above discussion, the origin of the two knick points has to be sought in a more complex evolution of the Rhone profile.The existence of two phases of sea lowering during the Messinian crisis have been suggested by (Clauzon et al., 1996) . A first phase with a minimum of 400 m of sea lowering occurs before a second phase of 150 ky with >1000 m of lowering (Beaudoin et al., 1997).

Taking into account this point and the duration of the Messinian crisis (5.8–5.35 My; Beaudoin et al., 1997), a first phase of 300 ky with a minimum of 400 m of sea lowering and a second phase of 150 ky with an

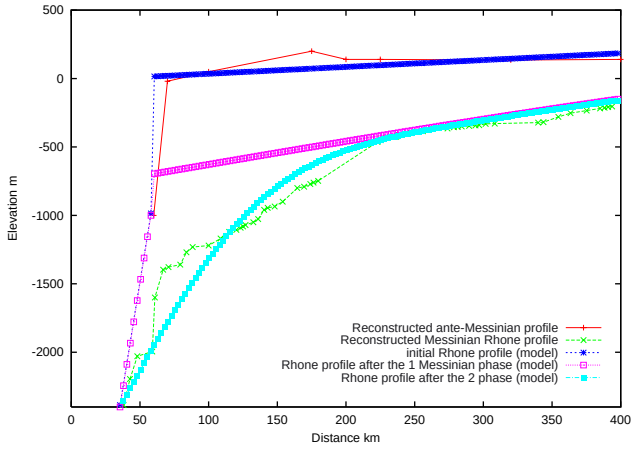

Fig. 11. Comparison between the reconstructed profile and the model. 2 phases are simulated with the model. In the first phase a lowering of 700 m during 300 ky happened ($k = 350\,000\ m^2$/year). In the second phase a lowering of 1500 m during 150 ky happened ($k = 20\,000\ m^2$/year).

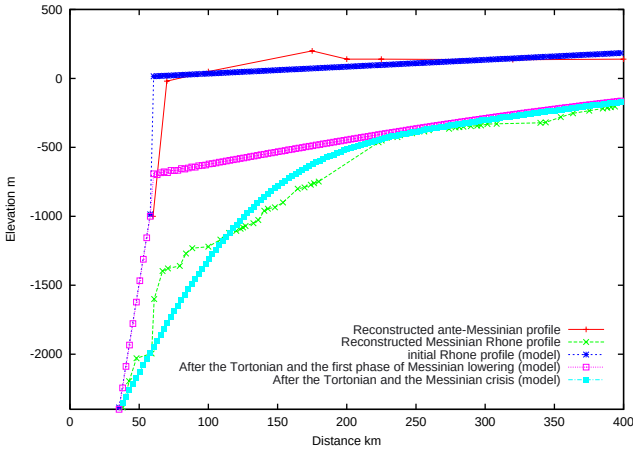

Fig. 12. Comparison between the reconstructed profile and model. 3 phases are simulated with the model. In the first phase two lowering of 100 m during 200 ky each one happened ($k = 170\,000\ m^2$/year). In the second phase a lowering of 600 m during 300 ky happened ($k = 170\,000\ m^2$/year). In the third phase a lowering of 1700 m during 150 ky happened ($k = 20\,000\ m^2$/year).

amplitude of Mediterranean sea lowering > 1000 m were modeled. Assuming this hypothesis, the only possibility of the model to fit the reconstructed profile is to consider that the coefficient of erosion is not constant with time (Fig. 11). Thus, $k = 350\,000\ m^2$/y during the first phase of 700 m of lowering over 300 ky; and $k = 20\,000\ m^2$/y during the 150 ky of the second phase of 1500 m of lowering. The upstream part of the Rhone profile was at steady state before the second phase of lowering. The upstream part of the Rhone profile is independent of the second phase of regression. Nevertheless there is no physical explication to the important variation with time of K: climatic variations can't explain this variation alone.

6.1. Influence of duration

6.1.1. Influence of duration of the Messinian crisis

Considering that the Messinian salinity crisis could have had a greater duration (5.96–5.33 million years) as suggested by Krijgsman et al. (1999), the consequences of a first lowering over a longer period could be tested. In this case, the profile is at steady state after 480 ky for a value of $k = 120\,000\ m^2$/y. Under this assumption, there is a diminution of the variation of the coefficient of erosion between the first ($k = 120\,000\ m^2$/y over 480 ky) and the second phase ($k = 20\,000\ m^2$/y over 150 ky).

6.1.2. Influence of the Tortonian erosion

It can also be considered that the ante-Messinian profile is older than supposed above. In this case, the possible influence of the sea level history before the Messinian crisis must be investigated, requiring study of the consequences of the Tortonian erosion.

During the upper Miocene, the Tortonian high sea level is considered as a starting point for the Rhone valley. The Tortonian high stand in the Rhone Valley has been identified in the Valence region (Demarcq, 1970). After the highest Tortonian sea level, two sea level lowerings of around 100 m were identified in Spain before the Messinian crisis (Franssen et al., 1998). Each lasted approximately 200 ky. The results of Franssen et al. (1998) exceed the value of the Tortonian sea level lowering proposed by Haq et al. (1987), establishing a maximum value of the possible Tortonian erosion. Furthermore, the Tortonian Rhone valley is not necessary located in the same place as the Messinian valley. Lateral migration of the valley may have happened.

If the ante-Messinian profile is older than the Messinian crisis, the Rhone River could have begun to incise its valley during the Tortonian. The model starts from the same initial profile as in the preceding simulation, but we consider that the incision began during the Tortonian sea low level and so the profile is eroded over more time (400 ky of Tortonian erosion, 300 ky during the first Messinian erosion and 150 ky for the second phase of the Messinian erosion). The possible effects of the Tortonian erosion on the profile are not negligible but remain limited (< 100 m) in comparison to the Messinian erosion. The profile is in steady state after the first Messinian phase. Considering the influence of Tortonian erosion reduces the variations of the coefficient of erosion k. Thus, $k = 170\,000\ m^2$/y during the Tortonian and the first Messinian phase, and $k = 20\,000\ m^2$/y for the second Messinian phase (Fig. 12).

6.2. Influence of Messinian isostatic deformation

In the first modeling test the Messinian defomation was not considered because of scarce infomation about

it. The possibility of Messinian uplift has been suggested by Clauzon (1982) near Pierrelatte and also at Saint-Desirat. The total crustal uplift that happened during the Messinian crisis in the Rhone valley has been eroded.

6.2.1. *Influence of messinian erosion*

Here, the isostatic deformation resulting from the deep valley incision is quantified, supposing that the Rhone valley incision occurs only during the Messinian crisis. Isostatic deformation was modeled for seven valley sections along the Messinian Rhone profile (Fig. 1).

In the downstream part, the Messinian isostatic deformation in the valley is between 50 ($D=10^{24}$ N m) and 500 m ($D=10^{20}$ N m) (Fig. 13). The uplift deformation is between 10 and 120 m for the valley section 2 and between 30 and 200 m for the valley section 3 (Figs. 13 and 14). For the valley section 4, near Pierrelatte, the Messinian isostatic uplift is between 20 and 170 m (Fig. 14).

In the upstream part, the Messinian isostatic uplift is between some meters and 25 m for the valley section 5 (Fig. 15). For the valley sections 6 and 7, the Messinian isostatic deformation is negligible (Figs 15 and 16).

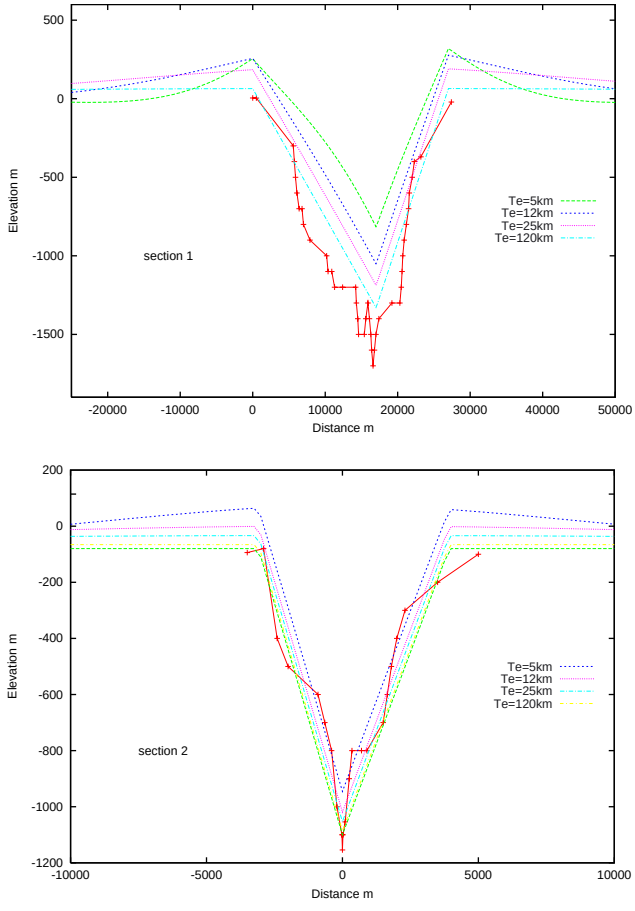

Fig. 13. Effect of isostasy on the Rhone valley just after incision (sections 1 and 2).

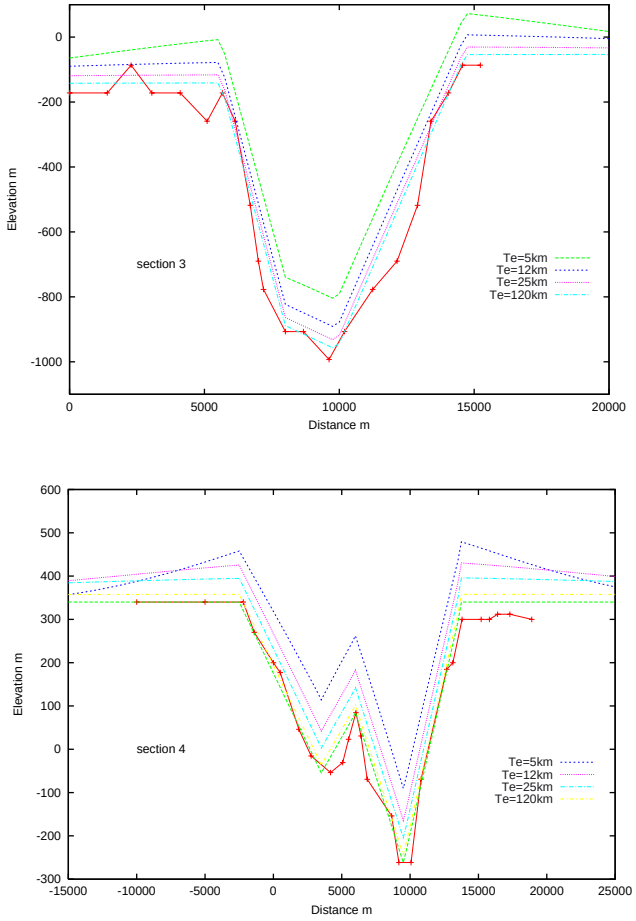

Fig. 14. Effect of isostasy on the Rhone valley just after incision (sections 3 and 4).

6.2.2. *Influence of Mediterranean sea unloading*

Mediterranean Sea lowering during the Messinian crisis produced unloading of the lithosphere (Norman and Chase, 1986). This unloading produced a regional uplift of the shoreline. Mediterranean Sea lowering was modeled from the south of France to North Africa using a schematic basin 700 km large and 2.5 km deep. Two hypotheses for the Mediterranean Sea lowering were tested because of the uncertainty of this parameter: (1) lowering of 2500 m, (2) lowering of 1500 meters.

For the first hypothesis, an uplift of more than 500 m of the Mediterranean basin and an uplift of the shoreline between 30 and 300 m were obtained (Fig. 17). The location of the deformation due to Mediterranean Sea unloading is between 30 km ($D=10^{20}$ N m) and 180 km from the shoreline ($D=10^{24}$ N m). For the second hypothesis, the Mediterranean basin uplift is between 300 and 500 m. The deformation on the coastline is between 30 and 225 m (Fig. 17).

6.2.3. *Influence of Pliocene infilling*

After the Messinian crisis, sediment loading happened during the Plio-Quaternary. The consequence of the

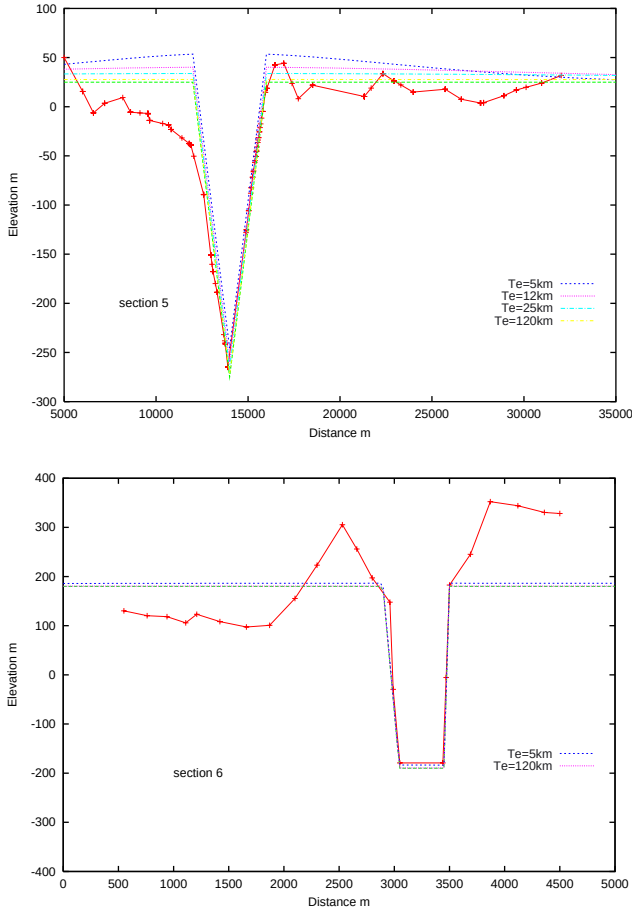

Fig. 15. Effect of isostasy on the Rhone valley just after incision (sections 5 and 6).

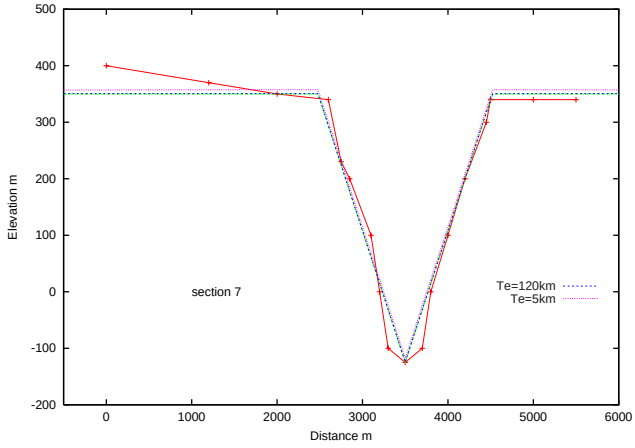

Fig. 16. Effect of isostasy on the Rhone valley just after incision (section 7). Saint-Desirat.

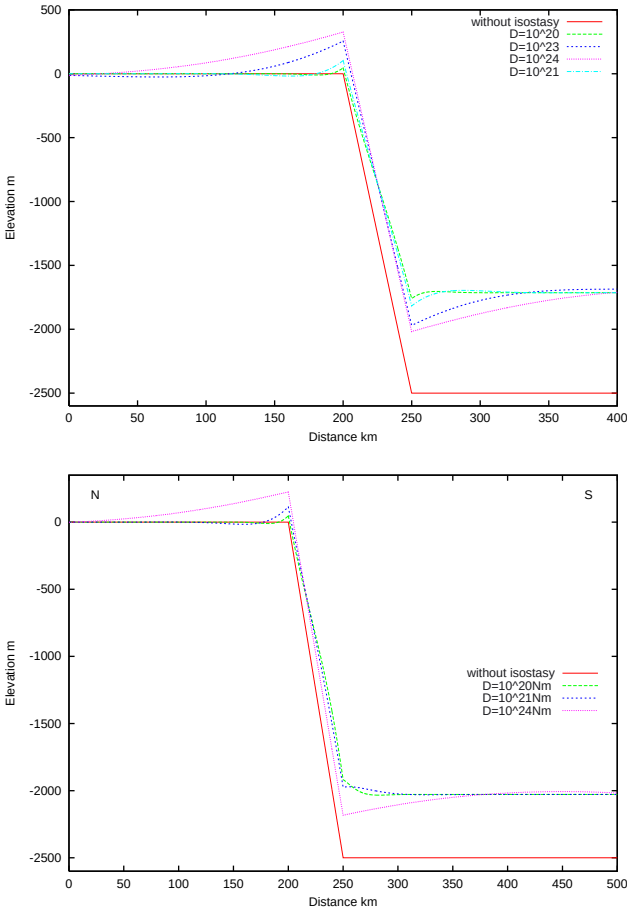

Fig. 17. Deformation resulting from Mediterranean sea unloading. We suppose that during the messinian the lowering is (1) of 2500 m, (2) of 1500 m.

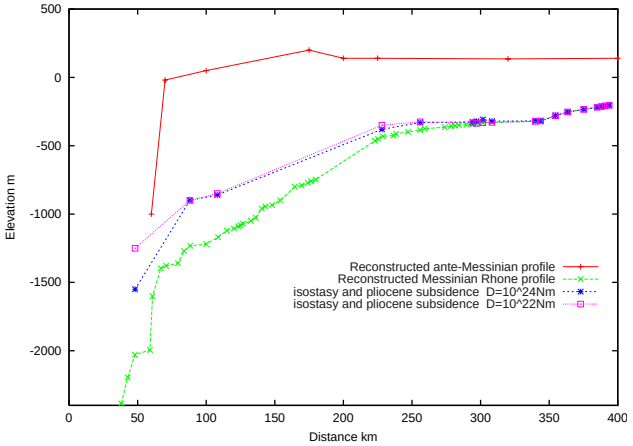

Fig. 18. Rhone river profile reconstructed taking into account post-messinian deformation, downstream subsidence included, and messinian isostatic deformation, for flexural rigidity of $D = 10^{22}$ N m and $D = 10^{24}$ N m.

Pliocene infilling is a regional subsidence in the downstream part of the Rhone river profile. The Pliocene subsidence due to the valley infilling is of the same order as the Messinian uplift due to valley incision, except in Pierrelatte where the valley has not been completely filled. This is the minimum subsidence of the downstream part of the Rhone River profile.

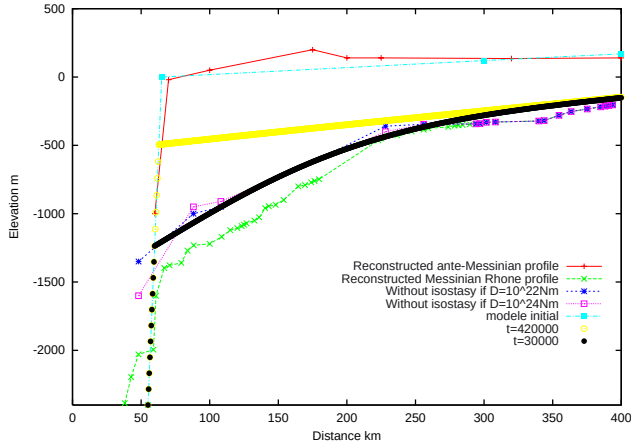

Fig. 19. Consequences of the two phase of the Mediterranean sea lowering on the messinian Rhone river profile. Comparison between modelling and the reconstructed messinian Rhone river profile.

The reconstructed Messinian Rhone profile is proposed in Fig. 18. In this profile, the post-Messinian deformations, downstream subsidence included, but also the effect of isostatic deformations due to valley incision and sea unloading has been taken into account.

The reconstructed profile seems compatible with a sea lowering of around 1500 m. The Messinian Rhone River profile has two knick points as before reconstruction, but the Pierrelatte knick point is less important after taking into account Messinian deformations.

A new comparison between the model and the reconstructed Messinian Rhone profile is proposed. A constant value is adopted for the coefficient of erosion ($k = 700\,000$) for the two phases of sea lowering. The first phase involved a sea level lowering of 600 m over 400 ky, whereas the second phase involved lowering of 1400 m over 50 ky (Fig. 19). A good fit of the reconstructed Messinian Rhone River profile was obtained.

7. Discussion and conclusion

Different tests on the parameters influencing the results of the modeling show that the Rhone profile cannot be explained only by lithological changes or changes in discharge resulting from the influence of tributaries. There is no possibility to fit data considering a constant coefficient of erosion if the Messinian isostatic deformation is not taken into account. A limited pre-Messinian incision cannot explain the variation of the coefficient of erosion.

The two phases for the Mediterranean Sea lowering during the Messinian crisis proposed by Beaudoin et al. (1997) are compatible with the model results. The amplitude of the first phase of sea level lowering during the Messinian is between 600 and 700 m, whereas the second one is between 1300 and 1700 m. 'The thermic subsidence of the lithosphere may have affected the southern part of the Rhone profile. A precise quantification of the effect of the thermic subsidence of the lithosphere in this region is necessary to improve the evaluation of the second Mediterranean sea lowering during the Messinian crisis.' The duration of the second Messinian phase is 50 ky, whereas the duration of the first phase is around 400 ky.

The morphology of the shoreline during the Messinian crisis has been affected by deformation due to isostatic response to the valley incision and the sea unloading. This change may have produced changes in the fluvial system and influenced the lateral migration of some rivers. The study of another Messinian river profile, such as the Nile, could give the opportunity to give a more precise quantification of the sea level lowering, but also to quantify the mechanical properties of the lithosphere determining the flexural rigidity necessary to construct compatible river profiles among all the Messinian rivers.

Acknowledgements

I. Cojan, O. Stab and J. Colson are gratefully acknowledged for their comments on a first version of this paper. I thank Juan C. Braga and an anonymous reviewer for their constructive comments.

References

Allen, P.A., Densmore, A.L., 2000. Sediment flux from an uplifting fault block. Basin Research 12, 367–380.

Ballesio, R., 1972. Étude stratigraphique du Pliocène Rhodanien. Documents des Laboratoires de Géologie de la faculté des sciences de Lyon, edited by Université Claude Bernard, 53, 333p.

Baumard, B., 2001. Valorisation des données pour l'étude de la crise messinienne dans le Gard rhodanien et la moitié Est de la France. Ph.D. Thesis, Ecole des Mines de Paris, 265 p.

Beaudoin, B., Accarie, H., Berger, E., Brulhet, J., Cojan, I., Haccard, D., Mercier, D., Mouroux, B., Clauzon, G., 1997. Caractérisation de la "crise messinienne" et de la réinondation pliocène. Atlas des posters, Journées scientifiques ANDRA (Agence nationale pour la gestion des déchets radioactifs), 20–21.

Begin, Z.B., Meyer, D.F., Schumm, S.A., 1981. Development of longitudinal profiles of alluvial channels in response to base-level lowering. Earth Surface Processes and Landforms 6, 49–68.

Bellaiche, G., Coutellier, V., Droz, L., Orsolini, P., Mear, Y., 1984. Detailed morphology of the Continental Margin of Western Provence (France). Compte Rendue Academie des Sciences Serie II 298 (19), 851–856.

Bellaiche, G., Coutellier, V., Droz, L., 1988. Sedimentary structure and evolution of the lower slope and continental rise off the Gulf of Lyons and western Provence since the late Miocene. Compte rendue Academie des Sciences Serie II 307, 957–963.

Carslow, M.S., Jaeger, D.A., 1959. Conduction of Heat in Solids. Clarendon Press, Oxford 510 p.

Cita, M.B., 1973. Mediterranean Evaporites: Paleontological arguments for a deep-basin dessication model. In: Drooger, C.W. (Ed.), Messinian events in the Mediterranean. North Holland Publishing, Amsterdam, pp. 206–228.

Clauzon, G., 1982. The messinian rhone canyon as a definite proof of the "dessicated deep-basin model". Bulletin Société Géologique de France XXIV, 597–610.

Clauzon, G., Suc, J-P., Gautier, F., Gautier, A., Berger, A., Loutre, M-F., 1996. Alternate interpretation of the messinian salinity crisis; controversy resolved? Geology 24, 363–366.

Colson, J., Stab, O., Beaudoin, B., 2000. Modélisation d'un incision future de type messinien du système Rhône-Cèze. Rapport ANDRA (Agence nationale pour la gestion des déchets radioactifs), D RP 0ARM 97-016/A, Paris.

Culling, W.E.H., 1960. Analytical theory of erosion. Journal of Geology 68, 336–344.

Demarcq, G., 1970. Etude stratigraphique du miocène rhodanien. Mèmoires du Bureau de Recherches Géologiques et Minières 61 (Paris), 257.

Durand Delga, M., 1980. La mediterranee occidentale: etapes de sa genese et problemes structuraux liess a celle-ci. Memoire, Société Géologique de France 10, 203–224.

Franssen, E.K., Goldstein, R.H., Farr, R., 1998. Quantitative controls on location and architecture of carbonate depositional sequences upper Miocene, Cabo de Gata, SE Spain. Journal of Sedimentary Research 68, 283–298.

Guennoc, P., Gorini, C., Mauffret, A., 2000. Geological history of the Gulf of Lyons: mapping the Oligocene-Aquitanian rift and Messinian surface. Géologie de la France 3, 67–97.

Haq, B.U., Hardenbol, J., Vail, P.R., 1987. Chronology of fluctuating sea levels since the Triassic (250 ma to the present). Science 235, 1156–1167.

Howard, A.D., Dietrich, W.E., Seidl, M.A., 1994. Modeling fluvial erosion on regional to continental scales. Journal of Geophysical Research 99 (B7), 13971–13986.

King, G., Ellis, M., 1990. The origin of large scale local uplift in extensional regions. Nature 348, 689–693.

Kooi, H., Beaumont, C., 1994. Escarpment evolution on high-elevation rifted margins: insights derived from a surface processes model that combines diffusion, advection, and reaction. Journal of Geophysical Research 99 (B6), 12191–12209.

Kooi, H., Cloethingh, S., Burrus, J., 1992,. Lithospheric necking and regional isostasy at extensional Basins 1. Subsidence and gravity modeling with an application to the Gulf of Lyons margin (SE France). Journal of Geophysical research 97 (B12), 17553–17571.

Krijgsman, W., Hilgen, F.J., Raffi, I., Sierro, F.J., Wilson D, S., 1999. Chronology, causes and progression of the Messinian salinity crisis. Nature 400, 652–655.

Le Pichon, X., Pautot, G., Auzende, J.M., Olivet, J.L., 1971. La Mediterranee occidentale. Biochronologie, correlations avec les formations marines et echanges intercontinentaux. Earth Planetary Science Letters 13, 145–152.

Malinverno, A., Cafiero, M., Ryan, W.B.F., Cita, M.B., 1981. Distribution of the Messinian sediments and erosional surfaces beneath the Tyrrhenian Sea: geodynamic implications. Oceanologica Acta 4, 489–495.

Mandier, P., 1988. Le Relief de la moyenne vallée du Rhone au Tertiaire et au Quaternaire. Document du Bureau de recherches géologiques et minières 151 (Paris), 654.

Mauffret, A., 1979. Etude geodynamique de la marge des iles Baleares. Memoirs Société geologie France, N.S. LVI (1 3 2), 94.

Montgomery, D.R., 1994. Valley incision and the uplift of mountain peaks. Journal of Geophysical Research 99 (B7), 13913–13921.

Nearing, M.A., Nicks, A.D., 1998. Evaluation of the water erosion prediction project (WEPP) model for hillslopes. In: Modelling Soil Erosion by Water, NATO ASI Series Kluwer, Dordrecht Vol. 55, pp. 43-53.

Norman, S.E., Chase, C.G., 1986. Uplift of the shores of the western Mediterranean due to Messinian desiccation and flexural isostasy. Nature 322, 450–451.

Pazzaglia, F.J., Gardner, T.W., Merritz, D.J., 1998. Bedrock fluvial incision and longitudinal profile development over geologic time scales and determined by fluvial terraces. In: Tinkler, K.J., Wohl, E.E. (Eds.), Rivers Over Rock: Fluvial Processes in Bedrock Channels, Vol. 107. American Geophysical Union Monograph, Washington, pp. 207–235.

Pelletier, J.D., Turcotte, D.L., 1997. Synthetic stratigraphy with a stochastic diffusion model of fluvial sedimentation. Journal of Sedimentary Research 67, 1060–1067.

Perrin, M., Roudier, P., Peroche, B., 1993. Computer aided 3D erosional modelling operated on geologically diversified folded and faulted terrains. Geoinformatics 4, 161–166.

Rouchy, J.M., 1981. La génèse des évaporites messiniennes de Méditerrannée. Ph.D. Thesis, Muséum de Université du Paris 6, France.

Ryan, W.B.F, Cita, M.B., 1978. The nature and distribution of Messinian erosional surfaces. Indicators of a several-kilometers-deep Mediterranean in the Miocene. Marine Geology 7, 193–230.

Schlupp, A., Clauzon, G., Avouac, J-P., 2001. Post-Messinian movement along the Nimes Fault: implication for the seismotectonics of Provence (France). Bulletin Societe Géologique de France 172, 697–711.

Thomas, W.A., 1982. Mathematical Modelling of Sediment Movement. In: Hey, R.D., Bathurst, J.C., Thorne, C.R. (Eds.), Gravel-bed Rivers. John Wiley, New York, pp. 487–508.

Veldkamp, A., van Dijke, J.J., 2000. Simulating internal and external controls on fluvial terrace stratigraphy: a qualitative comparison with the Maas record. Geomorphology 33, 225–236.

Weissel, J.K., Karner, G.D., 1989. Flexural uplift of rift flanks due to mechanical unloading of the lithosphere during extension. Journal of Geophysical Research 94, 13919–13950.

Willgoose, G., Bras, R.L., Rodriguez-Iturbe, I., 1991. A coupled channel network growth and hillslope evolution model (2. Theory). Water Resources Research 27, 1671–1684.